

Virtual-Voltage Partition-Based Approach to Mixed-Integer Optimal Power Flow Problems

Chin-Yao Chang Sonia Martínez Jorge Cortés

Abstract—This paper deals with optimal power flow (OPF) problems with discrete variables that capture binary decisions about network topology configurations and capacitor bank settings. We adopt a semidefinite programming formulation for the OPF problem which, however, remains nonconvex due to the presence of discrete variables and bilinear products between the decision variables. To tackle the latter, we introduce a novel physically-inspired, virtual-voltage approximation that leads to provable lower and upper bounds on the solution of the original problem. To deal with the exponential complexity caused by the discrete variables, we introduce a graph partition-based algorithm which breaks the problem into several parallel mixed-integer subproblems of smaller size. Simulations on the IEEE 30, 118, 300 bus test cases demonstrate the high degree of accuracy and affordable computational requirements of our approach.

I. INTRODUCTION

Mixed integer programming (MIP) arises in optimal power flow (OPF) problems involving switching control decisions, such as transformer tap settings, transmission line connections, and capacitor bank switching. The optimization of OPF problems with continuous and discrete variables has the potential to yield significant benefits in efficiency and reliability, but the complexity of solving such highly non-convex problems makes achieving this goal difficult. System operators usually select switching control laws *offline* to handle contingency situations and maintain system stability. In this way, they decouple the decisions about discrete variables from the OPF problem: once discrete controls have been specified, OPF focuses on generation cost or loss minimization. These observations motivate our focus on the co-optimization of discrete decisions and OPF.

Literature review: The works [2], [3] provide surveys on the solution of OPF problems with discrete variables. Many of the methods employed to solve OPF problems have been extended to deal with MIP-OPF problems, e.g., particle swarm optimization [4], [5] and genetic algorithms [6]. Transmission line switching or network topology reconfiguration commonly serves as a corrective mechanism in response to system contingencies see [7], [8] and references therein. In [9], [10], linearized OPF, also known as DCOPF, is used for the fast co-optimization of network topology and OPF. Despite its relative low complexity, DCOPF may lead, especially in congested systems, to poor solutions that can even result in voltage collapse [11], [12]. The work [13] proposes quadratic convex (QC) relaxations for the MIP-OPF problem, which provides more accurate results than DCOPF, while still retaining a fast computation time. Recent studies [13], [14] show that methods

based on semidefinite programming (SDP) convex relaxations of ACOPF may lead to better solutions than DCOPF and QC. However, how to handle discrete variables in the context of SDP is challenging and not fully understood. The challenges stem from not only from the integer-valued nature of these variables, but also from the presence of bilinear terms involving the product of discrete decision variables with continuous ones, reflecting the impact on the physical modeling of the line being connected. The paper [14] uses a lift-and-branch-and-bound procedure to deal with the SDP formulation of MIP-OPF problems, but has still exponential complexity in the worst case due to the nature of the branch-and-bound procedure. The work [15] also uses SDP to solve MIP-OPF problems, where bilinear terms associated to line connections are addressed by assuming certain nominal network topology and bilinear terms of other discrete decision variables are dealt with using the McCormick relaxation [16].

Statement of contributions: We consider the co-optimization of transmission line switching and optimal power flow. We introduce the SDP convex relaxation of the OPF problem and add discrete variables that can model transmission line and capacitor bank switching. Our contributions are twofold. First, we introduce a novel way of dealing with the nonconvexity coming from the presence of bilinear terms, which we term virtual-voltage approximation. Our approach is based on introducing virtual voltage variables for the terminal nodes of each switchable line and impose physically-meaningful constraints on them. We show that this approach leads to sound bounds on the optimal power losses and individual flows of the switchable lines, and provides lower and upper bounds on the optimal value of the original problem. Our second contribution deals with the nonconvexity coming from the discrete variables. We build on the virtual-voltage approximation to propose a graph partition-based algorithm that significantly reduces the computational complexity of solving the original problem. This algorithm uses the values of the optimal dual variables from the virtual voltage method to define a weighted network graph, which is then partitioned with a minimum weight edge-cut set. The algorithm breaks the original network into sub-networks so as to minimize the correlation between the solutions to the optimization problem on each sub-network. Finally, the algorithm solves a mixed-integer SDP problem on each sub-network in parallel and combines them to reconstruct the solution of the original problem. We implement the proposed algorithms on IEEE 30, 118, and 300 bus test cases, and compare them with available approaches from the literature to illustrate their superior performance regarding convergence to the optima and computation time.

C.-Y. Chang, S. Martínez, and J. Cortés are with the Department of Mechanical and Aerospace Engineering, UC San Diego.

A preliminary version of this work appeared as [1] at the 2017 Allerton Conference on Communications, Control, and Computing.

II. PRELIMINARIES

This section introduces basic concepts used in the paper¹.

1) *Graph Theory*: We review basic notions of graph theory following [17]. A graph is a pair $\mathcal{G} = (\mathcal{N}, \mathcal{E})$, where $\mathcal{N} \subseteq \mathbb{N}$ is the set of nodes and $\mathcal{E} \subseteq \mathcal{N} \times \mathcal{N}$ is the set of edges. A *self-loop* is an edge that connects a node to itself. The graph is *undirected* if $\{i, k\} = \{k, i\} \in \mathcal{E}$. A *path* is a sequence of nodes such that any two consecutive nodes correspond to an edge. The graph is *connected* if there exists a path between any two nodes. An *orientation* of an undirected graph is an assignment of exactly one direction to each of its edges. A graph is *simple* if it does not have self-loops or multiple edges connecting any pair of nodes. Throughout the paper, we limit our discussion to undirected, simple graphs. A *vertex-induced subgraph* of \mathcal{G} , written $\mathcal{G}[\mathcal{N}_s] = (\mathcal{N}_s, \mathcal{E}_s)$, satisfies $\mathcal{N}_s \subseteq \mathcal{N}$ and $\mathcal{E}_s = \mathcal{E} \cap (\mathcal{N}_s \times \mathcal{N}_s)$. An *edge cut set* is a subset of edges which, if removed, disconnects the graph. A *weighted graph* is a graph where each branch $\{i, k\}$ has a weight, $w_{ik} \in \mathbb{R}_+$. Given the edge weights $w \in \mathbb{R}_+^{|\mathcal{E}|}$, the *adjacency matrix* A has $A(i, k) = A(k, i) = w_{ik}$ if $\{i, k\} \in \mathcal{E}$, and $A(i, k) = 0$ otherwise. The *degree matrix* D is a diagonal matrix such that $D(i, i) = \sum_{k, \{i, k\} \in \mathcal{E}} w_{ik}$. The *Laplacian matrix* is $L = D - A$. The Laplacian matrix is positive semidefinite, with zero as an eigenvalue and multiplicity equal to the number of connected components in the graph. The *Fiedler vector* is the eigenvector associated with the second smallest eigenvalue of L . An *n-partition* of a connected $\mathcal{G} = (\mathcal{N}, \mathcal{E}, A)$ divides \mathcal{G} into a number of n connected vertex-induced subgraphs, $\mathcal{G}[\mathcal{V}_i]$, such that $\bigcup_{i=1}^n \mathcal{V}_i = \mathcal{N}$ and $\mathcal{V}_i \cap \mathcal{V}_k = \emptyset$ for all $i \neq k$. An *n-optimal partition* of $\mathcal{G} = (\mathcal{N}, \mathcal{E}, A)$ is an n -partition of \mathcal{G} with $\sum_{\{i, k\} \in \mathcal{E}_c} w_{ik}$ minimized, where $\mathcal{E}_c = \mathcal{E} \setminus (\bigcup_{i=1}^n \mathcal{V}_i \times \mathcal{V}_i)$. *Spectral graph partitioning* partitions a connected graph \mathcal{G} into two vertex-induced subgraphs, $\mathcal{G}[\mathcal{N}_1]$ and $\mathcal{G}[\mathcal{N}_2]$, where \mathcal{N}_1 and \mathcal{N}_2 are the nodes corresponding to the positive and non-positive entries of the Fiedler vector, respectively.

2) *McCormick Relaxation of Bilinear Terms*: The McCormick envelopes [16] provide linear relaxations for optimization problems that involve bilinear terms. Consider a bilinear term xy on the variables $x, y \in \mathbb{R}$, for which there exist upper and lower bounds, $\underline{x} \leq x \leq \bar{x}$, $\underline{y} \leq y \leq \bar{y}$. The McCormick relaxation consists of substituting in the optimization problem the term xy by its surrogate $v \in \mathbb{R}$ and adding the following McCormick envelopes on v ,

$$v \geq \underline{x}y + x\underline{y} - \underline{x}\underline{y}, \quad v \geq \bar{x}y + x\bar{y} - \bar{x}\bar{y}, \quad (1a)$$

$$v \leq \bar{x}y + x\underline{y} - \bar{x}\underline{y}, \quad v \leq \underline{x}\bar{y} + x\bar{y} - \underline{x}\bar{y}. \quad (1b)$$

Constraints (1) are tight, in the sense that each plane in (1) is tangent to the bilinear-constraint manifold at two boundary lines. The convex polyhedron in the variables (x, y, v) encloses the actual bilinear-constraint manifold.

¹We use the following notation. We denote by \mathbb{N} , \mathbb{R} , \mathbb{R}_+ , and \mathbb{C} the sets of positive integer, real, positive real, and complex numbers, resp. We denote by $|\mathcal{N}|$ the cardinality of \mathcal{N} . For a complex number $a \in \mathbb{C}$, we let $|a|$ and $\angle a$ be the complex modulus and angle of a , and its real and imaginary parts are $\Re(a)$ and $\Im(a)$. We let $\|v\|$ denote the 2-norm of $v \in \mathbb{C}^n$. Let $\mathbb{S}_+^n \subset \mathbb{C}^{n \times n}$ and $\mathcal{H}^n \subset \mathbb{S}_+^n$ be the set of positive semidefinite and n -dimensional Hermitian matrices, resp. For $A \in \mathbb{C}^{n \times n}$, we let A^* and $\text{Tr}\{A\}$ denote its conjugate transpose and trace, resp. We let $A(i, k)$ denote the (i, k) th element of A .

III. PROBLEM STATEMENT

We begin with the formulation of the OPF problem over an electrical network and its SDP convex relaxation following [18]. Then, we introduce binary variables for the co-optimization of line switching and capacitor banks, leading to the problem formulation of interest in this paper.

Consider an electrical network with generation buses \mathcal{N}_G , load buses \mathcal{N}_L , and electrical interconnections described by an undirected edge set \mathcal{E} . Let $\mathcal{N} = \mathcal{N}_G \cup \mathcal{N}_L$ and denote its cardinality by N . We denote the phasor voltage at bus i by $V_i = E_i e^{j\theta_i}$, where $E_i \in \mathbb{R}$ and $\theta_i \in [-\pi, \pi)$ are the voltage magnitude and phase angle, respectively. For convenience, $V = \{V_i \mid i \in \mathcal{N}\}$ denotes the collection of voltages at all buses. The active and reactive power injections at bus i are given by the power flow equations

$$P_i = \text{Tr}\{Y_i V V^*\} + P_{D_i}, \quad Q_i = \text{Tr}\{\bar{Y}_i V V^*\} + Q_{D_i}, \quad (2)$$

where $P_{D_i}, Q_{D_i} \in \mathbb{R}$ are the active and reactive power demands at bus i , and $Y_i, \bar{Y}_i \in \mathcal{H}^N$ are derived from the admittance matrix $\mathbf{Y} \in \mathbb{C}^{N \times N}$ as follows

$$Y_i = \frac{e_i e_i^T \mathbf{Y}^* + e_i e_i^T \mathbf{Y}}{2}, \quad \bar{Y}_i = \frac{(e_i e_i^T \mathbf{Y})^* - e_i e_i^T \mathbf{Y}}{2j}. \quad (3a)$$

Here $\{e_i\}_{i=1, \dots, N}$ denotes the canonical basis of \mathbb{R}^N . The OPF problem also involves the box constraints

$$\begin{aligned} \underline{V}_i^2 &\leq |V_i|^2 \leq \bar{V}_i^2, \quad \forall i \in \mathcal{N}, \\ \underline{P}_i &\leq P_i \leq \bar{P}_i, \quad \underline{Q}_i \leq Q_i \leq \bar{Q}_i, \quad \forall i \in \mathcal{N}, \\ |V_i - V_k|^2 &\leq \bar{V}_{ik}, \quad \forall \{i, k\} \in \mathcal{E}, \end{aligned} \quad (4)$$

where \bar{V}_{ik} is the upper bound of the voltage difference between buses i, k , and \underline{V}_i and \bar{V}_i are the lower and upper bounds of the voltage magnitude at bus i , respectively. All $\underline{P}_i, \underline{Q}_i, \bar{P}_i, \bar{Q}_i$, are defined similarly. The objective function is typically given as a quadratic function of the active power,

$$\sum_{k \in \mathcal{N}_G} c_{i2} P_i^2 + c_{i1} P_i, \quad (5)$$

where $c_{i2} \geq 0$, and $c_{i1} \in \mathbb{R}$. The OPF problem is the minimization over (5) subject to (2) and (4). Such optimization is non-convex due to the quadratic terms on V . To address this, one can equivalently define $W = V V^* \in \mathcal{H}^N$ (or $W \in \mathcal{H}^N$ and $\text{rank}(W) = 1$) as the decision variable (note all the terms in (2), (4) and (5) are quadratic in V). Dropping the rank constraint on W makes the OPF problem convex, giving rise to the SDP convex relaxation,

$$(P1) \quad \min_{W \succeq 0} \sum_{i \in \mathcal{N}_G} c_{i2} P_i^2 + c_{i1} P_i,$$

subject to

$$P_i = \text{Tr}\{Y_i W\} + P_{D_i}, \quad \forall i \in \mathcal{N}, \quad (6a)$$

$$Q_i = \text{Tr}\{\bar{Y}_i W\} + Q_{D_i}, \quad \forall i \in \mathcal{N}, \quad (6b)$$

$$\underline{P}_i \leq P_i \leq \bar{P}_i, \quad \underline{Q}_i \leq Q_i \leq \bar{Q}_i, \quad \forall i \in \mathcal{N}, \quad (6c)$$

$$\underline{V}_i^2 \leq \text{Tr}\{M_i W\} \leq \bar{V}_i^2, \quad \forall i \in \mathcal{N}, \quad (6d)$$

$$\text{Tr}\{M_{ik} W\} \leq \bar{V}_{ik}, \quad \forall \{i, k\} \in \mathcal{E}, \quad (6e)$$

where $M_i, M_{ik} \in \mathcal{H}^N$ are defined so that $\text{Tr}\{M_i W\} = |V_i|^2$ and $\text{Tr}\{M_{ik} W\} = |V_i - V_k|^2$.

We are interested in solving the OPF problem with discrete variables that model topology reconfigurations via line switching. Assume that an additional set of edges, $\mathcal{E}_s \subset (\mathcal{N} \times \mathcal{N}) \setminus \mathcal{E}$, could be added to the network $\mathcal{G} = (\mathcal{N}, \mathcal{E})$. Topological changes could make the system more robust and reduce generation cost. For each line $\{i, k\} \in \mathcal{E}_s$, we define a binary variable $\alpha_{ik} \in \{0, 1\}$, and we say the line is connected if $\alpha_{ik} = 1$ and disconnected otherwise. If $\alpha_{ik} = 1$, then the power flow from node i to k through edge $\{i, k\} \in \mathcal{E}_s$ is

$$P_{ik} = \text{Tr}\{Y_{ik}W\}, \quad Q_{ik} = \text{Tr}\{\bar{Y}_{ik}W\}, \quad (7)$$

where $Y_{ik}, \bar{Y}_{ik} \in \mathbb{C}^{N \times N}$ are defined as follows: all entries are prescribed to be zero except the ones defined by²

$$Y_{ik}(i, i) = \Re(y_{ik}), \quad Y_{ik}(i, k) = Y_{ik}^*(i, k) = -y_{ik}/2, \\ \bar{Y}_{ik}(i, i) = \Im(y_{ik}), \quad \bar{Y}_{ik}(i, k) = \bar{Y}_{ik}^*(i, k) = -j \cdot y_{ik}/2.$$

Here $y_{ik} \in \mathbb{C}$ is the admittance of line $\{i, k\}$. Taking (7) into account, the active and reactive power of each node become

$$P_i = \text{Tr}\{Y_i W\} + P_{D_i} + \sum_{k \in \mathcal{N}_{i,s}} \alpha_{ik} P_{ik}, \quad (8) \\ Q_i = \text{Tr}\{\bar{Y}_i W\} + Q_{D_i} + \sum_{k \in \mathcal{N}_{i,s}} \alpha_{ik} Q_{ik},$$

where $\mathcal{N}_{i,s} := \{k \mid \{i, k\} \in \mathcal{E}_s\}$. Given $\alpha \in \{0, 1\}^{|\mathcal{E}_s|}$, we use **(P1)- α** to refer to the OPF problem solved with the network topology with extra lines as determined by α .

We are interested in solving what we call **(P2)**, which is the optimization **(P1)** with constraints (6a) and (6b) replaced by (7) and (8). In addition to optimizing the power flows, this corresponds to also selecting the optimal set of lines to connect among the ones in \mathcal{E}_s . The problem **(P2)** is non-convex for two reasons: the binary variables α_{ik} and the bilinear products of α_{ik} and W . The first problem can be addressed using existing integer-programming solvers [19], [15]. The McCormick relaxation described in Section II-2 is the standard way to deal with the second problem. In this paper, we instead provide alternative routes to address each of these problems for the optimization **(P2)**.

Remark III.1. (OPF with capacitor bank switching). The formulation above focuses on the co-optimization of OPF and line switching, but it can also accommodate capacitor-bank switching. This generalization entails an equation similar to (8) to adjust the reactive power injection as follows

$$Q_i = \text{Tr}\{\bar{Y}_i W\} + Q_{D_i} - C_i \alpha_s \sqrt{W(i, i)}, \quad (9)$$

where $C_i \in \mathbb{R}_+$, and α_s can take multiple positive integer values. The latter can be equivalently represented via binary variables. The last term in (9) entails non-convex bilinear products of decision variables, as described above. \square

IV. VIRTUAL-VOLTAGE APPROXIMATION OF BILINEAR TERMS

We introduce here a novel way to deal with the bilinear terms in **(P2)** which we term *virtual-voltage approximation*. We start by noting that every binary variable α only appears in

the bilinear products in (8) together with another continuous variable W . If we convexify the binary variables by having them take values in $[0, 1]$, then we can interpret each bilinear term corresponding to $\{i, k\} \in \mathcal{E}_s$ as a line power flow from i to k , with the magnitude bounded by what W indicates. Following this reasoning, if the direction of power flow of every line $\{i, k\} \in \mathcal{E}_s$ was known, then the bilinear term would no longer be an issue. For example, if we knew that $P_{ik} = \text{Tr}\{Y_{ik}W\} \in \mathbb{R}_+$ and $Q_{ik} = \text{Tr}\{\bar{Y}_{ik}W\} \in \mathbb{R}_+$, then we could define new variables, $\hat{P}_{ik} \in \mathbb{R}$ and $\hat{Q}_{ik} \in \mathbb{R}$, replacing $\alpha_{ik}P_{ik}$ and $\alpha_{ik}Q_{ik}$ in (8), respectively, and impose

$$0 \leq \hat{P}_{ik} \leq P_{ik}, \quad 0 \leq \hat{Q}_{ik} \leq Q_{ik}. \quad (10)$$

This would eliminate the bilinear terms and the only remaining non-convexity would be that the physical feasible solution should satisfy $\hat{P}_{ik} \in \{0, P_{ik}\}$ and $\hat{Q}_{ik} \in \{0, Q_{ik}\}$. In general, however, the direction of power flow of the lines $\{i, k\} \in \mathcal{E}_s$ is not known a priori and, hence, the trivial convex constraints (10) for the relaxation are no longer valid.

A. Convex Relaxation Via Virtual Voltages

Our idea to approximate each bilinear term builds on defining a virtual voltage for the terminal nodes of the line and impose constraints on them to make sure they have physical sense. We make this precise next. Let $\hat{\mathcal{E}}_s$ be an arbitrary orientation of \mathcal{E}_s . To define the virtual voltages, and in keeping with the SDP approach, for each $\{i, k\} \in \hat{\mathcal{E}}_s$ we introduce a two-by-two positive semidefinite matrix $U_{ik} \in \mathbb{S}_+^2$. This matrix encodes physically meaningful voltages at the terminal nodes if its rank is one, namely, $U_{ik} = u_{ik}u_{ik}^\top$, with $u_{ik}(1)$ and $u_{ik}(2)$ corresponding to the voltages of nodes i and k , respectively. For convenience, we introduce $\hat{M} = \begin{bmatrix} 1 & -1 \\ -1 & 1 \end{bmatrix}$ and impose the following constraints on U_{ik}

$$U_{ik}(1, 1) \leq \text{Tr}\{M_i W\}, \quad (11a)$$

$$U_{ik}(2, 2) \leq \text{Tr}\{M_k W\}, \quad (11b)$$

$$\text{Tr}\{\hat{M}U_{ik}\} \leq \text{Tr}\{M_{ik}W\}. \quad (11c)$$

Constraints (11a) and (11b) ensure that the voltage magnitudes of i and k derived from U_{ik} are no bigger than the ones from W . Constraint (11c) ensures that the voltage difference between nodes i and k computed from U_{ik} is less than the corresponding difference from W . Therefore, if the matrix U_{ik} has rank one, constraints (11) ensure that we obtain physically meaningful and feasible voltage values.

Let $\hat{Y}_{ik} \in \mathbb{C}^{2 \times 2}$ be the principal sub-matrix of Y_{ik} by only keeping the rows and columns associated with nodes i and k . We define $\hat{\bar{Y}}_{ik}$ similarly. We replace $\alpha_{ik}P_{ik}$ and $\alpha_{ik}Q_{ik}$ in (8) by $\text{Tr}\{\hat{Y}_{ik}U_{ik}\}$ and $\text{Tr}\{\hat{\bar{Y}}_{ik}U_{ik}\}$, respectively. We now have all the elements necessary to convexify **(P2)** as follows

$$\textbf{(P3)} \quad \min_{W \succeq 0, U_{ik} \succeq 0 \ \forall \{i,k\} \in \hat{\mathcal{E}}_s} \sum_{i \in \mathcal{N}_G} \left(c_{i2}P_i^2 + c_{i1}P_i \right),$$

subject to (6c)-(6e), (11), and

$$P_i = \text{Tr}\{Y_i W\} + P_{D_i} + \sum_{k \in \mathcal{N}_{i,s}} \text{Tr}\{\hat{Y}_{ik}U_{ik}\}, \quad (12a)$$

$$Q_i = \text{Tr}\{\bar{Y}_i W\} + Q_{D_i} + \sum_{k \in \mathcal{N}_{i,s}} \text{Tr}\{\hat{\bar{Y}}_{ik}U_{ik}\}. \quad (12b)$$

²We omit charging susceptance, tap ratio and phase shift of transformers for simplicity.

Remark IV.1. (OPF with capacitor bank switching – continued). The formulation (P3) can also be employed to relax the bilinear terms involved in capacitor banks, cf. Remark III.1. Let $\alpha_{s,i} \in \{0,1\}$ be the binary control of a capacitor bank. We replace $\alpha_{s,i}\sqrt{W(i,i)}$ in (9) by a new variable $x_i \in \mathbb{R}_+$ and impose the following constraints on x_i

$$\begin{aligned} U_{s,i}(1,2) + U_{s,i}(2,1) &= x_i, \\ U_{s,i}(1,1) &\leq \text{Tr}\{M_i W\}, \quad U_{s,i}(2,2) \leq 1/4, \end{aligned}$$

where $U_{s,i}$ is a two-by-two real-valued positive semidefinite matrix. In this way, $\alpha_{s,i} = 0$ if $U_{s,i} = 0$, and $\alpha_{s,i} = 1$ when the inequalities become equalities. \square

Each optimal solution $U_{ik}^{\text{opt}_3}$ of (P3) has a dominant eigenvalue, much larger than the other one. To formally state the result, let $W_{ik}^{\text{opt}_3} \in \mathcal{H}^2$ denote the principal sub-matrix of the optimum W^{opt_3} of (P3) obtained by removing from W^{opt_3} all columns and rows except the ones corresponding to i and k . We use the spectral decomposition to rewrite $U_{ik}^{\text{opt}_3}$ as

$$U_{ik}^{\text{opt}_3} = a_{ik}[u_i, u_k]^\top [u_i^*, u_k^*] + [u_i, -u_k]^\top [u_i^*, -u_k^*],$$

where $u_i \in \mathbb{C}$, $u_k \in \mathbb{C}$, and $a_{ik} \geq 1$ is the condition number of $U_{ik}^{\text{opt}_3}$. Lemma IV.2 establishes a useful lower bound on a_{ik} .

Lemma IV.2. (Lower bound on the condition number). For all $\{i, k\} \in \hat{\mathcal{E}}_s$, the optima of (P3) has

$$\frac{|u_i|^2 + |u_k|^2 + 2\Re(u_i u_k^*)}{\bar{V}_{ik} - (|u_i|^2 + |u_k|^2 - 2\Re(u_i u_k^*))} \leq a_{ik}. \quad (13)$$

Proof. By constraint (11c) and (6e), we have

$$\begin{aligned} (a_{ik} + 1)(|u_i|^2 + |u_k|^2) - 2(a_{ik} - 1)\Re(u_i u_k^*) \\ \leq a_{ik} \text{Tr}\{M_{ik} W^{\text{opt}_3}\} \leq a_{ik} \bar{V}_{ik} \end{aligned}$$

Lemma IV.2 follows by rearranging the inequality above. \square

For all practical purposes, the result of Lemma IV.2 implies that the matrix $U_{ik}^{\text{opt}_3}$ specifies well-defined virtual voltages at the terminal nodes, as we explain next.

Remark IV.3. (Optimal solutions have well-defined virtual voltages). Using Lemma IV.2, we justify that the optimal solution $U_{ik}^{\text{opt}_3}$ has a dominant eigenvalue as follows. The denominator of (13) is always non-negative due to (11c). The order of the denominator of (13) is at most 10^{-2} as $\bar{V}_{ik} \approx 10^{-2}$ in most test cases. On the other hand, when the virtual voltage satisfies $\text{Tr}\{\hat{M} U_{ik}^{\text{opt}_3}\} \approx \text{Tr}\{M_i W^{\text{opt}_3}\}$ or $\text{Tr}\{\hat{M} U_{ik}^{\text{opt}_3}\} \approx \text{Tr}\{M_k W^{\text{opt}_3}\}$, then the numerator is lower bounded by a scalar close to one, as $\bar{V}_i \approx 1$. As a consequence, the fraction in (13) is usually bigger than 10^2 . Our simulations on IEEE 118 and 300 bus test cases confirm that a_{ik} is at least 100. \square

B. Physical Properties of the Convex Relaxation

The active and reactive power flows in (P3) on a switchable line $\{i, k\} \in \mathcal{E}_s$ are determined by U_{ik} according to

$$P_{ik}^{\text{opt}_3} = \text{Tr}\{\hat{Y}_{ik} U_{ik}^{\text{opt}_3}\}, \quad Q_{ik}^{\text{opt}_3} = \text{Tr}\{\hat{Y}_{ik} U_{ik}^{\text{opt}_3}\}. \quad (14)$$

The next result shows that the optimal power losses on each edge are bounded by the ones computed from W^{opt_3} .

Lemma IV.4. (Bounds on the sums of line active and reactive powers). If the line charging susceptance is zero for all $\{i, k\} \in \hat{\mathcal{E}}_s$, then the following inequalities hold

$$0 \leq P_{ik}^{\text{opt}_3} + P_{ki}^{\text{opt}_3} \leq \text{Tr}\{(Y_{ik} + Y_{ki}) W_{ik}^{\text{opt}_3}\}, \quad (15a)$$

$$0 \leq Q_{ik}^{\text{opt}_3} + Q_{ki}^{\text{opt}_3} \leq \text{Tr}\{(\bar{Y}_{ik} + \bar{Y}_{ki}) W_{ik}^{\text{opt}_3}\}. \quad (15b)$$

Proof. If the line charging susceptance is zero, then $Y_{ik} + Y_{ki}$ and $\bar{Y}_{ik} + \bar{Y}_{ki}$ take the following form

$$Y_{ik} + Y_{ki} = \hat{M} \Re(y_{ik}), \quad \bar{Y}_{ik} + \bar{Y}_{ki} = \hat{M} \Im(-y_{ik}).$$

Since both $\Re(y_{ik})$ and $\Im(-y_{ik})$ are non-negative, the result of Lemma IV.4 follows from (11c) and the equalities (14). \square

We next seek to upper bound the individual flows $|P_{ik}|$ and $|P_{ki}|$. Our next result shows that, under certain conditions for (P3), stronger properties hold on the active power retrieved from the optimal solution $U_{ik}^{\text{opt}_3}$ and W^{opt_3} .

Proposition IV.5. (Bounds on directional power flow). Let $w_i = \sqrt{W^{\text{opt}_3}(i,i)}$ for each $i \in \mathcal{N}$. Assume $\{i, k\} \in \hat{\mathcal{E}}_s$ is purely inductive and has zero charging susceptance, $|u_k| \in \{0, w_k\}$ and

$$w_i \geq w_k/2, \quad w_k \geq w_i/2. \quad (16)$$

Then the following inequalities hold

$$|P_{ik}^{\text{opt}_3}| \leq |\text{Tr}\{Y_{ik} W_{ik}^{\text{opt}_3}\}|, \quad |P_{ki}^{\text{opt}_3}| \leq |\text{Tr}\{Y_{ki} W_{ik}^{\text{opt}_3}\}|. \quad (17)$$

Proof. If $\{i, k\}$ is purely inductive and has zero charging susceptance, then

$$\hat{Y}_{ik} = \frac{1}{2} \begin{bmatrix} 0 & y_{ik}^* \\ y_{ik} & 0 \end{bmatrix}, \quad \hat{Y}_{ki} = \frac{1}{2} \begin{bmatrix} 0 & y_{ik} \\ y_{ik}^* & 0 \end{bmatrix}.$$

Note that only the off-diagonal entries of \hat{Y}_{ik} and \hat{Y}_{ki} are non-zero, making $P_{ik}^{\text{opt}_3} = -P_{ki}^{\text{opt}_3}$ and $|\text{Tr}\{Y_{ik} W_{ik}^{\text{opt}_3}\}| = |\text{Tr}\{Y_{ki} W_{ik}^{\text{opt}_3}\}|$. If $|u_k| = 0$, (17) follows as $P_{ik}^{\text{opt}_3} = -P_{ki}^{\text{opt}_3} = 0$. It is then enough to show that if $|u_k| = w_k$, $|P_{ik}^{\text{opt}_3}| \leq |\text{Tr}\{Y_{ik} W_{ik}^{\text{opt}_3}\}|$. We show it by contradiction. If $|P_{ik}^{\text{opt}_3}| > |\text{Tr}\{Y_{ik} W_{ik}^{\text{opt}_3}\}|$, then $|u_i| > 0$ and $|u_i||u_k| \sin(\theta_{ik}^u) > w_i w_k \sin(\theta_{ik}^w)$, where $\theta_{ik}^w = \angle W_{ik}^{\text{opt}_3}$, and θ_{ik}^u is the angle difference between u_i and u_k . Using (11a), we define $\xi_i \geq 1$ such that $\xi_i |u_i| = w_i$, and rewrite the inequality as $|\sin(\theta_{ik}^u)| > \xi_i |\sin(\theta_{ik}^w)|$. Then,

$$|\cos(\theta_{ik}^u)| < \sqrt{1 - \xi_i^2 \sin^2(\theta_{ik}^w)}. \quad (18)$$

Rewriting (11c) as a function of w_i, w_k, ξ_i ,

$$0 \leq w_i^2 - \frac{w_i^2}{\xi_i^2} - 2w_i w_k \left(\cos(\theta_{ik}^w) - \frac{1}{\xi_i} \cos(\theta_{ik}^u) \right), \quad (19)$$

where we use $|u_k| = w_k$ in the inequality. Using (18), the RHS of (19) is less than

$$w_i^2 - \frac{w_i^2}{\xi_i^2} - 2w_i w_k \left(\cos(\theta_{ik}^w) - \frac{1}{\xi_i} \sqrt{1 - \xi_i^2 \sin^2(\theta_{ik}^w)} \right). \quad (20)$$

The derivative (20) with respect to ξ_i is

$$\frac{2w_i^2}{\xi_i^3} - \frac{4w_i w_k}{\sqrt{1 - \xi_i^2 \sin^2(\theta_{ik}^w)}} - \frac{2w_i w_k}{\xi_i^2} \sqrt{1 - \xi_i^2 \sin^2(\theta_{ik}^w)}. \quad (21)$$

The first two elements summed up to a non-positive value due to (16). We then conclude that (21) is non-positive with $W_{ik}^{\text{opt}_3}$ given and fixed. Therefore, (20) is non-positive for all ξ_i because it is zero when $\xi_i = 1$ and is non-increasing. But (20) is strictly larger than the RHS of (19), contradicting (19). \square

Condition (16) holds for most existing power systems [20]. An analogous result holds by restricting u_i instead.

Proposition IV.6. (Bounds on directional power flow. II). *If $\{i, k\} \in \hat{\mathcal{E}}_s$ is purely inductive and has zero charging susceptance, $|u_i| \in \{0, w_i\}$ and \bar{V}_{ik} is sufficiently small such that (16) holds, then (17) follows.*

The proof of Proposition IV.6 is analogous to that of Proposition IV.5 and therefore we omit it. Similar bounds as (17) follow for reactive power if the sum of the cosine terms in the bracket of (19) is non-negative (however, in general, this is not the case). In addition, more involved, inequalities as (17) hold for the general impedance case, but we do not pursue them here. Propositions IV.5 and IV.6 show that, when the diagonal entries of $U_{ik}^{\text{opt}_3}$ are at the boundary points of their constraints, (P3) eliminates the bilinear terms on the active line power flow of (P2) in the same way as (10). The difference between the relaxations is that there is no need in (P3) to know the direction of line power flow a priori, as opposed to (10).

C. Reconstructed Solution to the MIP-OPF Problem

We note that the ratio of the voltage magnitudes derived from $U_{ik}^{\text{opt}_3}$ and $W_{ik}^{\text{opt}_3}$ provides an approximation of the discrete variables α_{ik} in (8) as

$$\hat{\alpha}_{ik} = \text{Tr}\{U_{ik}^{\text{opt}_3}\} / \text{Tr}\{W_{ik}^{\text{opt}_3}\}. \quad (22)$$

Note that $\hat{\alpha} \in [0, 1]^{|\hat{\mathcal{E}}_s|}$ because of (11). If we round the entries of $\hat{\alpha}$ to the closest number in $\{0, 1\}$, we obtain a candidate solution $\hat{\alpha}_r \in \{0, 1\}^{|\hat{\mathcal{E}}_s|}$ to (P2). The following result, whose proof is straightforward, states the relationship between (P2) and (P3) based on the rounded solution $\hat{\alpha}_r$.

Proposition IV.7. (Properties of the reconstructed solution). *The optimal values of (P1)- $\hat{\alpha}_r$, (P2), and (P3) satisfy $p_1^{\text{opt}} \geq p_2^{\text{opt}} \geq p_3^{\text{opt}}$. Moreover, if $p_1^{\text{opt}} = p_3^{\text{opt}}$, then the optimal solution of (P1)- $\hat{\alpha}_r$, W_1^{opt} , combined with $\hat{\alpha}_r$, is an optimal solution of (P2).*

Note that even if $\hat{\alpha} = \hat{\alpha}_r \in \{0, 1\}^{|\hat{\mathcal{E}}_s|}$, p_3^{opt} does not necessarily equal p_2^{opt} . The reason is that (22) computes $\hat{\alpha}_{ik}$ from the diagonal of $U_{ik}^{\text{opt}_3}$, and hence we can not conclude any equality for the off-diagonal elements of $U_{ik}^{\text{opt}_3}$ and $W_{ik}^{\text{opt}_3}$. Hence, even if $\hat{\alpha} \in \{0, 1\}^{|\hat{\mathcal{E}}_s|}$, the optimal solution of (P3) does not necessarily lie in the feasible region of (P2).

Remark IV.8. (Comparison with the McCormick relaxation). We explain how we implement the McCormick relaxation on the problem (P2) for comparison purposes. For each $\{i, k\} \in \hat{\mathcal{E}}_s$, we define new variables $\hat{P}_{ik}, \hat{Q}_{ik} \in \mathbb{R}$ to substitute the bilinear terms $\alpha_{ik}P_{ik}, \alpha_{ik}Q_{ik}$, respectively. Then, we impose constraints of the form (1) on the new variables based on $\alpha_{ik} \in \{0, 1\}$ and upper and lower bounds of active/reactive line power flow, $\bar{P}_{ik}, \bar{Q}_{ik} \in \mathbb{R}_+$, $\underline{P}_{ik} = -\bar{P}_{ik}, \underline{Q}_{ik} =$

$-\bar{Q}_{ik}$. If these bounds are far from the actual optimal line power flows, this can significantly affect the quality of the solution obtained by the McCormick relaxation, a point that we illustrate later in our simulations, along with rationale for how to select them. In contrast, the proposed relaxation (P3) is not sensitive to those line power bounds, as the virtual voltages are bounded by the power computed from W . Additionally, the variables \hat{P}_{ik} and \hat{Q}_{ik} in the McCormick relaxation are loosely tied to the decision variable W , whereas (P3) introduces constraints (11a)-(11c) enforcing a stronger physical connection between the virtual voltages and W . \square

V. PARTITION-BASED MIP-OPF ALGORITHM

In general, the solution to the convex relaxation (P3) of the MIP-OPF problem introduced in Section IV provides a lower bound on its optimal value, cf. Proposition IV.7. Here, we discuss how to refine the reconstructed solution to better approximate the solution of the original optimization problem. One approach consists of using the branch-and-bound algorithm [21] and relying on (P3) to generate the required branch lower bounds in its execution. However, this approach can easily become intractable as the number of switchable lines grows because of the large number of cases where (P3) must be executed. To address the exponential complexity, we propose an alternative method, described as follows:

[Informal description]: The algorithm partitions the network graph into smaller components to break the original problem into subproblems of smaller size. To do this, we view the disconnection of a line as a perturbation on the constraint (6c). This is natural, in the sense that the disconnection changes the active and reactive power injections of the terminal nodes, which in turn may cause the constraints to be violated. Hence, we partition the graph so that the correlation between the solutions to the optimization problem on each of the resulting subgraphs is minimized. The idea is that, if the optimal solution in each subgraph minimally violates the constraints that connect them to other graphs' solutions, then, when put together, the reconstructed solution to (P2) would be of better quality.

Algorithm 1 formally presents the partition-based MIP-OPF algorithm. Next, we describe in detail each of its steps.

Algorithm 1 Partition-Based MIP-OPF Algorithm

- 1: **Compute** the optimal solution W^{opt} of (P3)
 - 2: **Construct** graph reduction \mathcal{G}_r (Section V-1)
 - 3: **Assign** adjacency matrix to \mathcal{G}_r (Section V-2)
 - 4: **Compute** cut set \mathcal{E}_c to partition \mathcal{G}_r into n subgraphs (Section V-2)
 - 5: **Solve** integer optimization problem (P4) on each subgraph to find α_p^{opt} (Section V-3)
 - 6: **Solve** (P1)- α_p^{opt} (Section V-4)
-

1) *Graph reduction:* This is a step prior to graph partitioning which is motivated by the following observation. The graph partitioning should not result in nodes connected

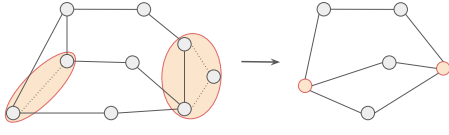


Fig. 1: Graph reduction. Nodes connected by \mathcal{E}_s are collapsed into one node. The dash lines denote edges in \mathcal{E}_s ; the solid lines denote the edges in \mathcal{E} .

by a switchable line belonging to different subgraphs. This is because, if that were the case, then solving the OPF associated with each subgraph cannot capture how the switch in that specific line affects the optimal value of the original MIP-OPF problem. To address this, we ‘hide’ the nodes that are connected by \mathcal{E}_s to the partitioning algorithm that finds the edge cut \mathcal{E}_c so as to ensure $\mathcal{E}_s \cap \mathcal{E}_c = \emptyset$. Let $\mathcal{N}_s := \{i \in \mathcal{N} \mid \{i, k\} \in \mathcal{E}_s\}$ and let $\mathcal{N}_{s,i}$ be the set of nodes that are connected to node $i \in \mathcal{N}_s$ through a line in \mathcal{E}_s . All nodes in $\mathcal{N}_{s,i}$ are clustered as one representative node and all the edges connected to one of $\mathcal{N}_{s,i}$ are considered being connected to the representative node. This results in a graph $\mathcal{G}_r = ((\mathcal{N} \setminus \mathcal{N}_s) \cup \mathcal{V}, \mathcal{E}_r)$, where \mathcal{V} is the collection of representative nodes. Notice that $\mathcal{E}_r \subseteq \mathcal{E}$ and \mathcal{E}_r is a strict subset of \mathcal{E} if there is $\{i, k\} \in \mathcal{E}$ such that a path connecting nodes i and k exists in the graph $(\mathcal{N}, \mathcal{E}_s)$. Figure 1 illustrates the construction of \mathcal{G}_r and has $\mathcal{E}_r \subset \mathcal{E}$ as one edge of \mathcal{E} is dropped in the process of graph reduction.

Remark V.1. (Networks where all lines are switchable). The graph reduction step described above only makes sense when not all lines are switchable because otherwise, it results in a graph with a single node. Some works [22], [13], however, consider scenarios where all lines are switchable. For such scenarios, one can either skip the graph reduction step, or pre-select a set of lines that should remain non-switchable. We come back to this point in Section VI later. \square

2) *Graph partitioning:* Our next step is to find an edge cut set \mathcal{E}_c of the graph \mathcal{G}_r . In order to minimally affect the optimal value p^{opt} , the graph partitioning is based on the optimal dual variables of (P3). The optimum dual variables measure how the optimal value p_3^{opt} of (P3) changes with respect to the corresponding constraint. Formally, by taking the derivative of the Lagrangian of (P3), we have the following for $i \in \mathcal{N} \setminus \mathcal{N}_s$,

$$\underline{\lambda}_i^{\text{opt}_3} = \frac{\partial p_3^{\text{opt}}}{\partial \underline{P}_i}, \quad \bar{\lambda}_i^{\text{opt}_3} = \frac{\partial p_3^{\text{opt}}}{\partial \bar{P}_i}, \quad \underline{\gamma}_i^{\text{opt}_3} = \frac{\partial p_3^{\text{opt}}}{\partial \underline{Q}_i}, \quad \bar{\gamma}_i^{\text{opt}_3} = \frac{\partial p_3^{\text{opt}}}{\partial \bar{Q}_i},$$

and for $i \in \mathcal{V}$,

$$\underline{\lambda}_i^{\text{opt}_3} = \sum_{k \in \mathcal{N}_{s,i}} \frac{\partial p_3^{\text{opt}}}{\partial \underline{P}_k}, \quad \bar{\lambda}_i^{\text{opt}_3} = \sum_{k \in \mathcal{N}_{s,i}} \frac{\partial p_3^{\text{opt}}}{\partial \bar{P}_k},$$

$$\underline{\gamma}_i^{\text{opt}_3} = \sum_{k \in \mathcal{N}_{s,i}} \frac{\partial p_3^{\text{opt}}}{\partial \underline{Q}_k}, \quad \bar{\gamma}_i^{\text{opt}_3} = \sum_{k \in \mathcal{N}_{s,i}} \frac{\partial p_3^{\text{opt}}}{\partial \bar{Q}_k},$$

With this interpretation, we define edge weights as follows

$$A(i, k) = \begin{cases} \sum_{l \in \{i, k\}} \bar{\lambda}_l^{\text{opt}_3} + \underline{\lambda}_l^{\text{opt}_3} + \bar{\gamma}_l^{\text{opt}_3} + \underline{\gamma}_l^{\text{opt}_3}, & \{i, k\} \in \mathcal{E}_r, \\ 0, & \text{otherwise.} \end{cases}$$

Given the adjacency matrix A , we do an n -optimal partition on \mathcal{G}_r , which gives $\mathcal{G}_r[\mathcal{V}_1^0], \dots, \mathcal{G}_r[\mathcal{V}_n^0]$ with $\cup_{i=1}^n \mathcal{V}_i^0 =$

$(\mathcal{N} \setminus \mathcal{N}_s) \cup \mathcal{V}$. Since all the removed edges are in \mathcal{E} , we can use the same cut for the partition of \mathcal{G} : $\mathcal{G}[\mathcal{V}_1], \dots, \mathcal{G}[\mathcal{V}_n]$ with $\cup_{i=1}^n \mathcal{V}_i = \mathcal{N}$. Such partition ensures $\mathcal{E}_c \cap \mathcal{E}_s = \emptyset$. The intuition is that the cut minimally perturbs p^{opt} because it select edges with minimal weight for the weighted graph (\mathcal{G}, A) .

Finding the optimal cut set is NP-hard. There are algorithms [23], [24] that can approximate it in a few seconds for graphs of the order of a thousand nodes. However, they do not guarantee that the resulting subgraphs are connected. To ensure this property, we resort to spectral graph partitioning.

Theorem V.2. (Fiedler’s theorem of connectivity of spectral graph partitions). *The two subgraphs resulting from spectral graph partitioning on a connected graph are also connected.*

The proof is available in [25, Corollary 2.9]. To derive a n -partition, one can implement spectral graph partitioning recursively n times. Since we aim for subgraphs with similar size, each iteration applies spectral graph partitioning on the subgraph with the largest number of nodes. The most computationally expensive step in this process is the eigenvector computation, which only takes linear time, or $\mathcal{O}(n)$. This low complexity is reflected on the negligible computational time in our simulations. Even though this recursive spectral partitioning does not in general lead to an n -optimal partition, the sum of the weights of the edge cut set, $\sum_{\{i, k\} \in \mathcal{E}_c} A(i, k)$, can be upper bounded via Cheeger inequalities [26], [27].

3) *Integer optimization on subgraphs:* Given a n -partition $\{\mathcal{G}[\mathcal{V}_l]\}_{l=1}^n$, we define an optimization problem associated with each subgraph. This problem is a variant of (P2) that is convenient for the reconstruction of the solution of (P2) over the original \mathcal{G} . For subgraph l , let \mathcal{E}_l be its set of edges, $W_l \in \mathbb{S}_+^{|\mathcal{V}_l|}$ the decision variable, $\hat{\mathcal{E}}_{s,l}$ the set of switchable lines, and \mathcal{B}_l the set of nodes in \mathcal{V}_l that connects to at least one node of another subgraph. Each subgraph l solves

$$(\text{P4}) \quad \min_{W_l \succeq 0, \alpha_{ik} \in \{0, 1\}, \forall \{i, k\} \in \hat{\mathcal{E}}_{s,l}} \sum_{i \in \mathcal{N}_G \cap \mathcal{V}_l} (c_{i2} P_i^2 + c_{i1} P_i),$$

subject to

$$\underline{P}_i \leq P_i \leq \bar{P}_i, \quad \underline{Q}_i \leq Q_i \leq \bar{Q}_i, \quad \forall i \in \mathcal{V}_l,$$

$$\underline{V}_i^2 \leq \text{Tr}\{M_i W_l\} \leq \bar{V}_i^2, \quad \forall i \in \mathcal{V}_l,$$

$$\text{Tr}\{M_{ik} W_l\} \leq \bar{V}_{ik}, \quad \forall \{i, k\} \in \mathcal{E}_l.$$

For all $i \in \mathcal{V}_l \setminus \mathcal{B}_l$,

$$P_i = \text{Tr}\{Y_i W_l\} + P_{D_i} + \sum_{k, \{i, k\} \in \mathcal{E}_{s,i}} \alpha_{ik} \text{Tr}\{Y_{ik} W_{l,ik}\},$$

$$Q_i = \text{Tr}\{\bar{Y}_i W_l\} + Q_{D_i} + \sum_{k, \{i, k\} \in \mathcal{E}_{s,i}} \alpha_{ik} \text{Tr}\{\bar{Y}_{ik} W_{l,ik}\}.$$

For all $i \in \mathcal{B}_l$,

$$P_i = \text{Tr}\{Y_i W_l\} + P_{D_i} + \mathcal{P}_{l,i} + \sum_{k, \{i, k\} \in \mathcal{E}_{s,i}} \alpha_{ik} \text{Tr}\{Y_{ik} W_{l,ik}\},$$

$$Q_i = \text{Tr}\{\bar{Y}_i W_l\} + Q_{D_i} + \mathcal{Q}_{l,i} + \sum_{k, \{i, k\} \in \mathcal{E}_{s,i}} \alpha_{ik} \text{Tr}\{\bar{Y}_{ik} W_{l,ik}\},$$

where $\mathcal{P}_{l,i} = \sum_{k \in \mathcal{N} \setminus \mathcal{V}_l, \{i, k\} \in \mathcal{E}} P_{ik}^{\text{opt}_3}$ sums the active power flow from the solution of (P3), $\mathcal{Q}_{l,i}$ is defined similarly, and with a slight abuse of notation, all $M_i, M_{ik}, Y_i, \bar{Y}_i, Y_{ik}$ take proper dimensions matching W_l . Notice that (P4) is still NP-hard due to α_{ik} , but the number of switches $|\mathcal{E}_{s,i}|$ in each

partition is less than $|\mathcal{E}_s|$, and decreases with n . The addition of $\mathcal{P}_{l,i}$ and $\mathcal{Q}_{l,i}$ in (P4) accounts for the coupling between $\mathcal{G}[\mathcal{V}_i]$ and the other subgraphs. For each subgraph, these terms are constant and do not provide an exact approximation of the power exchanged between the subgraphs – since they do not take into account the dependency of the terminal voltage on the solutions determined on the other subgraphs. Therefore, putting together the solutions obtained for each subgraph may not result in a feasible solution of (P2), but rather a solution to (P2) with a perturbation on (6c). We address this next.

4) *Full SDP optimization with fixed topology*: In the last step, we define the candidate optimal switch $\alpha_p^{\text{opt}} \in \{0, 1\}^{|\mathcal{E}_s|}$ from the solutions of (P4) obtained in the previous step. With this in place, we solve (P1)- α_p^{opt} to obtain the candidate optimal solution W_p^{opt} and output $(\alpha_p^{\text{opt}}, W_p^{\text{opt}})$ as the reconstructed solution of (P2).

VI. SIMULATION STUDIES

In this section we illustrate the performance of the virtual-voltage approximation and the partition-based MIP-OPF algorithm on the IEEE 30, 118, and 300 bus test cases. We consider scenarios with either transmission line or capacitor bank switching. All simulations are done on a desktop with 3.5GHz CPU and 16GB RAM, using MATLAB and its CVX toolbox [28] to solve the convex optimization problems. In all our tables, “lower bound” refers to the optimal value of (P3) and “upper bound” refers to the optimal value of (P1)- α , where α is determined by the corresponding method.

A. Topology Design with a Subset of Switchable Lines

We first consider the IEEE 118 bus test system, which has 179 lines, and select 27 of them as switchable, following [22]. We include an additional cost function on the line power losses to avoid the optimal solution being the one with all edges connected. We implement the virtual-voltage approximation and compare its performance against the solution obtained from (P2) with the McCormick approximation (cf. Remark IV.8). For the latter, we use two different estimates on the upper bounds of the line power flows. In one case, we use the conservative bounds $\bar{P}_{ik} = -\underline{P}_{ik} = 5(\text{p.u.})$ and $\bar{Q}_{ik} = -\underline{Q}_{ik} = 5(\text{p.u.})$ for all $\{i, k\} \in \mathcal{E}_s$. These bounds come from solving the nominal IEEE 118 example with all 179 lines and taking the value of the largest line active/reactive power flow. In the other case, we set the tighter bounds $\bar{P}_{ik} = -\underline{P}_{ik} = 1(\text{p.u.})$ and $\bar{Q}_{ik} = -\underline{Q}_{ik} = 1(\text{p.u.})$ for all $\{i, k\} \in \hat{\mathcal{E}}_s$, based on our knowledge of the solution of the IEEE test nominal case, which results in better performance. The virtual-voltage approach yields discrete variables close to $\{0, 1\}$ and, in contrast, the McCormick relaxation has most of them around 0.5. Table I shows the values obtained by both approximations, and confirms that the virtual-voltage approach gives better solutions than the McCormick relaxation.

B. Topology Design When Every Line is Switchable

We examine the IEEE 118 and IEEE 300 bus test systems, with all lines considered as switchable. When implementing the partition-based MIP-OPF algorithm, and to avoid the problem described in Remark V.1, we select a set of lines

Virtual-voltage approximation	lower bound	150992
	upper bound	151040
McCormick relaxation w/ 5(p.u.) bounds	lower bound	144300
	upper bound	153657
McCormick relaxation w/ 1(p.u.) bounds	lower bound	146917
	upper bound	151373

TABLE I: Performance of the virtual-voltage approximation and the McCormick approximation on the IEEE 118 bus test case.

to remain non-switchable using the following policy: given a design parameter $p \in \mathbb{N}$, we rank all lines by the norm of their admittance in ascending order and select the first p as the set of switchable lines. The rationale for this selection is that each line with small admittance places a small correlation between its terminal nodes and, as a result, they are more likely to be disconnected. In our simulations, we use $p = 40$.

Table II shows the result of implementing on the IEEE 118 and IEEE 300 bus test cases the following methods: (i) the virtual-voltage approximation with all lines switchable; (ii) the virtual-voltage approximation with 40 switchable lines; and (iii) the partition-based MIP-OPF algorithm with 40 switchable lines. For the case with 40 switchable lines, one can see that the partition-based MIP-OPF algorithm refines the virtual-voltage approximation. We next compare the results in Table II with the QC relaxation method [13]. This method takes 10 hours to solve the MIP-OPF problem for both IEEE 118 and 300 bus test cases employing servers with 4334 CPUs and 64GB memory. The QC relaxation method converges to a near optimum with around 1% error for the IEEE 118 test case, while it is unable to provide a feasible solution for the IEEE 300 bus case. In contrast, solving (P3) with all lines switchable takes significantly less time for both cases (around 2min30sec and 1h30min, respectively) as shown in Table II. While the CVX toolbox does not give a feasible solution to (P1)- $\hat{\alpha}_r$ for the IEEE 300 bus case when all lines are switchable, the ones obtained by the virtual-voltage approximation and the partition-based MIP-OPF algorithm with 40 switchable lines are both close to the lower bound. We quantify their accuracy by upper bounding the percentage error with the true optimal solution using $(p_1^{\text{opt}} - p_{3,\text{all}}^{\text{opt}})/p_{3,\text{all}}^{\text{opt}} \cdot 100\%$.

C. Switch of Capacitor Banks

This simulation considers the IEEE 30 bus test case, with each node in $\mathcal{N}_c = \{10, 12, 15, 17, 20, 21, 23, 24, 29\}$ connected to a capacitor bank to support reactive power. Every capacitor only has two modes, with $C = 0.3(\text{p.u.})$. The OPF problem takes the form of (P1) with (6b) replaced by (9) for every node in \mathcal{N}_c , to which we still refer as (P2) with a slight abuse of notation.

Table III shows the result of implementing the following methods: (i) an SDP relaxation based on the McCormick approximation proposed in [15]; (ii) the virtual-voltage approximation implemented as described in Remark IV.1; and (iii) exhaustive search. Since we are dealing with capacitor banks, instead of (22), the approximation of the discrete variables is computed as $\hat{\alpha}_i = x_i^{\text{opt}}/\sqrt{W^{\text{opt}}(i, i)}$ for each $i \in \mathcal{N}_c$. As noted in the table, the proposed virtual-voltage approximation method outperforms the standard McCormick relaxation and is close to the true optimum. Among all $2^9 =$

		Optimal values		Bound on errors		Computation times (sec)	
		IEEE 118	IEEE 300	IEEE 118	IEEE 300	IEEE 118	IEEE 300
Virtual-voltage approximation w/ all lines switchable	lower bound	150791	1090397	0.36%	N/A	142.57	4859.62
	upper bound	151340	NaN				
Virtual-voltage approximation w/ 40 switchable lines	lower bound	151594	1086369	1.27%	0.52%	149.37	5023.90
	upper bound	152707	1096117				
Partition-based MIP-OPF w/ 40 switchable lines		152505	1092967	1.14%	0.24%	173	5055.88

TABLE II: Performance of the virtual-voltage approximation and the partition-based MIP-OPF algorithm on the IEEE 118 and IEEE 300 bus test cases. “NaN” means that CVX cannot find a feasible solution (even though the problem may still be feasible, see [29] for details).

512 possible combinations, the virtual-voltage approximation chooses the second-best solution, whereas the McCormick-based one chooses the seventh best.

SDP with McCormick relaxation	lower bound	1202
	upper bound	1270
Virtual-voltage approximation	lower bound	1202
	upper bound	1241
Exhaustive search		1238

TABLE III: Performance of the virtual-voltage approximation, an SDP relaxation based on the McCormick approximation [15], and exhaustive search on the IEEE 30 bus test case with capacitor bank switching.

VII. CONCLUSIONS

We have considered MIP-OPF problems with transmission line and capacitor bank switching. For these scenarios, the standard SDP relaxation of the problem remains non-convex because of the presence of bilinear terms and the discrete variables. We have proposed an approximation based on the introduction of virtual voltages to convexify the bilinear terms. We have also characterized several of its properties regarding physical interpretation and lower and upper bounds on the optimal value of the original problem. To handle the presence of the discrete variables, we have built on the virtual-voltage approximation to propose a graph partition-based algorithm that significantly reduces the computational complexity of solving the original problem. The high degree of accuracy and the reduction in computational complexity observed in simulations makes the proposed algorithms promising for MIP-OPF applications. Future work will incorporate other types of discrete controls, such as transformer tap changers and phase shifters, and investigate the design of distributed methods for solving MIP-OPF problems.

REFERENCES

- [1] C.-Y. Chang, S. Martínez, and J. Cortés, “Convex relaxation for mixed-integer optimal power flow problems,” in *Allerton Conf. on Communications, Control and Computing*, Monticello, IL, 2017, to appear.
- [2] J. Momoh, M. El-Hawary, and R. Adapa, “A review of selected optimal power flow literature to 1993. Part I: Nonlinear and quadratic programming approaches,” *IEEE Transactions on Power Systems*, vol. 14, no. 1, pp. 96–104, 1999.
- [3] S. Frank, I. Stepanavice, and S. Rebennack, “Optimal power flow: a bibliographic survey I,” *Energy Systems*, vol. 3, no. 3, pp. 221–258, 2012.
- [4] M. R. AlRashidi and M. E. El-Hawary, “A survey of particle swarm optimization applications in electric power systems,” *IEEE Transactions on Evolutionary Computation*, vol. 13, no. 4, pp. 913–918, 2009.
- [5] P. E. O. Yumbla, J. M. Ramirez, and C. A. Coello, “Optimal power flow subject to security constraints solved with a particle swarm optimizer,” *IEEE Transactions on Power Systems*, vol. 23, no. 1, pp. 33–40, 2008.
- [6] A. G. Bakirtzis, P. N. Biskas, C. E. Zoumas, and V. Petridis, “Optimal power flow by enhanced genetic algorithm,” *IEEE Transactions on Power Systems*, vol. 17, no. 2, pp. 229–236, 2002.
- [7] K. W. Hedman, S. S. Oren, and R. P. O’Neill, “A review of transmission switching and network topology optimization,” in *IEEE Power and Energy Society General Meeting*, Detroit, MI, 2011, electronic proceedings.
- [8] J. G. Rolim and L. J. B. Machado, “A study of the use of corrective switching in transmission systems,” *IEEE Transactions on Power Systems*, vol. 14, no. 1, pp. 336–341, 1999.
- [9] J. D. Fuller, R. Ramasra, and A. Cha, “Fast heuristics for transmission-line switching,” *IEEE Transactions on Power Systems*, vol. 27, no. 3, pp. 1377–1386, 2012.
- [10] P. A. Ruiz, J. M. Foster, A. Rudkevich, and M. C. Caramanis, “Tractable transmission topology control using sensitivity analysis,” *IEEE Transactions on Power Systems*, vol. 27, no. 3, pp. 1550–1559, 2012.
- [11] T. Potluri and K. W. Hedman, “Impacts of topology control on the ACOPF,” in *IEEE Power and Energy Society General Meeting*, San Diego, CA, 2012, electronic proceedings.
- [12] M. Soroush and J. D. Fuller, “Accuracies of optimal transmission switching heuristics based on DCOPF and ACOPF,” *IEEE Transactions on Power Systems*, vol. 29, no. 2, pp. 924–932, 2014.
- [13] H. Hijazi, C. Coffrin, and P. Van Hentenryck, “Convex quadratic relaxations for mixed-integer nonlinear programs in power systems,” *Mathematical Programming Computation*, vol. 9, no. 3, pp. 321–367, 2017.
- [14] J. Mareček, M. Mevissen, and J. C. Villumsen, “MINLP in transmission expansion planning,” in *Power Systems Computation Conference*, Genoa, Italy, 2016, electronic proceedings.
- [15] E. Briglia, S. Alaggia, and F. Paganini, “Distribution network management based on optimal power flow: Integration of discrete decision variables,” in *Annual Conference on Information Systems and Sciences*, Baltimore, MD, 2017, electronic proceedings.
- [16] G. P. McCormick, “Computability of global solutions to factorable nonconvex programs: Part I – convex underestimating problems,” *Mathematical programming*, vol. 10, no. 1, pp. 147–175, 1976.
- [17] F. Bullo, J. Cortés, and S. Martínez, *Distributed Control of Robotic Networks*, ser. Applied Mathematics Series. Princeton University Press, 2009, electronically available at <http://coordinationbook.info>.
- [18] J. Lavaei and S. H. Low, “Zero duality gap in optimal power flow problem,” *IEEE Transactions on Power Systems*, vol. 27, no. 1, pp. 92–107, 2012.
- [19] R. A. Jabr, R. Singh, and B. C. Pal, “Minimum loss network reconfiguration using mixed-integer convex programming,” *IEEE Transactions on Power Systems*, vol. 27, no. 2, pp. 1106–1115, 2012.
- [20] A. J. Wood and B. F. Wollenberg, *Power generation, operation, and control*. John Wiley & Sons, 2012.
- [21] I. E. Grossmann, “Review of nonlinear mixed-integer and disjunctive programming techniques,” *Optimization and Engineering*, vol. 3, no. 3, pp. 227–252, 2002.
- [22] P. A. Ruiz, A. Rudkevich, M. C. Caramanis, E. Goldis, E. Ntakou, and C. R. Philbrick, “Reduced MIP formulation for transmission topology control,” in *Allerton Conf. on Communications, Control and Computing*, Monticello, IL, 2012, pp. 1073–1079.
- [23] J. P. Hespanha, “An efficient Matlab algorithm for graph partitioning,” University of California, Santa Barbara, Tech. Rep., 2004.
- [24] A. Abou-Rjeili and G. Karypis, “Multilevel algorithms for partitioning power-law graphs,” in *International Parallel and Distributed Processing Symposium (IPDPS)*, Rhodes Island, Greece, 2006, electronic proceedings.
- [25] M. Fiedler, “A property of eigenvectors of nonnegative symmetric matrices and its application to graph theory,” *Czechoslovak Mathematical Journal*, vol. 25, no. 4, pp. 619–633, 1975.
- [26] F. Chung, “Laplacians of graphs and Cheeger’s inequalities,” in *Combinatorics, Paul Erdős is Eighty*, D. Miklós, V. T. Sós, and T. Szőnyi, Eds. Budapest, Hungary: János Bolyai Mathematical Society, 1996, vol. 2, pp. 157–172.
- [27] —, “Four Cheeger-type inequalities for graph partitioning algorithms,” *Proceedings of ICCM*, pp. 751–772, 2007.
- [28] M. Grant and S. Boyd, “CVX: Matlab software for disciplined convex programming, version 2.1,” Mar. 2014, available at <http://cvxr.com/cvx>.
- [29] M. Grant, S. Boyd, and Y. Ye, “CVX users guide,” 2009.